PROCEEDINGS OF SCIENCE

Spinodal Crumbling

Jan Steinheimer*
Nuclear Science Division, Lawrence Berkeley National Laboratory, Berkeley, California 94720, USA E-mail: jsfroschauer@lbl.gov

Jørgen Randrup
Nuclear Science Division, Lawrence Berkeley National Laboratory, Berkeley, California 94720, USA E-mail: jrandrup@lbl.gov

Extending a previously developed two-phase equation of state, we simulate head-on relativistic lead-lead collisions with fluid dynamics, augmented with a finite-range term, and study the effects of the phase structure on the evolution of the baryon density. For collision energies that bring the bulk of the system into the mechanically unstable spinodal region of the phase diagram, the density irregularities are being amplified significantly. We also present results for the associated clump size distribution.

8th International Workshop on Critical Point and Onset of Deconfinement, March 11 to 15, 2013
Napa, California, USA

*Speaker.

PoS(CPOD 2013)016

1. Introduction

Strongly interacting matter is expected to posses a rich phase structure. In particular, compressed baryonic matter may exhibit a first-order phase transition that persists up to a certain critical temperature [1] and experimental efforts are underway to search for evidence of this phase transition and the associated critical end point [2, 3, 4].

For these endeavors to be successful, it is important to identify observable effects that may serve as signals of the phase structure. This is a challenging task because the colliding system is relatively small, non-uniform, far from global equilibrium, and rapidly evolving. Therefore, to understand how the presence of a phase transition may manifest itself in the experimental observables, it is necessary to carry out dynamical simulations of the collisions with suitable transport models.

Many numerical simulations of high-energy nuclear collisions have employed ideal or viscous fluid dynamics which has the important advantage that the equation of state (EoS) appears explicitly. The focus up to now has mainly been on bulk observables and their dependence on a softening of the EoS. For this purpose, the instabilities associated with a first-order phase transition were usually removed by means of a Maxwell construction, thereby ensuring that bulk matter remains mechanically stable throughout the expansion.

However, when a first-order phase transition exists, a low-density confined phase (a hadronic resonance gas) may coexist thermodynamically with a high-density deconfined phase (a baryon-rich quark-gluon plasma) and, consequently, bulk matter prepared at intermediate densities would be unstable and seek to separate into the two coexisting phases. In a nuclear collision, when the dynamical evolution drives the bulk density into the phase coexistence region, the instabilities will be triggered. In particular, the spinodal instabilities [5, 6, 7, 8, 9] may generate a non-equilibrium evolution that in turn may generate observable fluctuations in the baryon density [10, 11, 12, 13] and the chiral order parameter [14, 15]. Furthermore, nucleation and bubble formation may also contribute towards the phase separation process.

In order to ascertain the degree to which these mechanisms may manifest themselves in actual nuclear collisions, we have performed numerical simulations with finite-density fluid dynamics, incorporating a gradient term in the local pressure [18]. This refinement emulates the finite-range effects that are essential for a proper description of the phase transition physics [5, 6, 8, 16]. In particular, the gradient term ensures that two coexisting bulk phases will develop a diffuse interface and acquire an associated temperature-dependent tension. Furthermore, of key importance to the present study, the gradient term also causes the dispersion relation for the collective modes in the unstable phase region to exhibit a maximum, as is a characteristic feature of spinodal decomposition [5]. Thus we employ a transport model that has an explicitly known two-phase equation of state and that treats the associated physical instabilities in a numerically reliable manner.

2. The Equation of State

In order to obtain a suitable equation of state, we employ the method developed in Ref. [8]. Thus we work (at first) in the canonical framework and, for a given T, we obtain the free energy density $f_T(\rho)$ in the phase coexistence region by performing a suitable spline between two ideal-

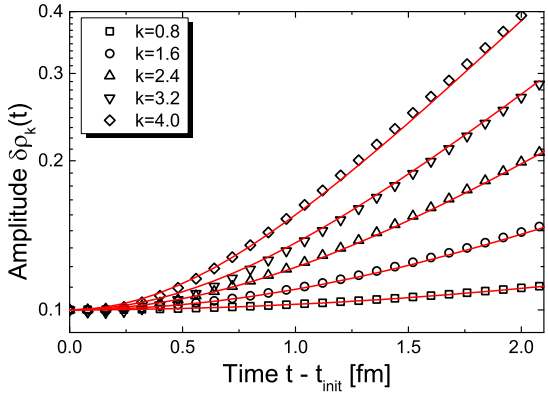

Figure 1: The growth of harmonic density undulations inside the spinodal region as obtained with standard ideal fluid dynamics, shown by the symbols for various values of the wave number k, together with the resulting fits to the expected analytical form (3.5), shown by the continuous curves.

ized systems (either a gas of pions and interacting nucleons or a bag of gluons and quarks) held at that temperature. In Ref. [8] the focus was restricted to subcritical temperatures, $T < T_{\rm crit}$, so for each T the spline points were adjusted so the resulting $f_T(\rho)$ would exhibit a concave anomaly, *i.e.* there would be two densities, $\rho_1(T)$ and $\rho_2(T)$, for which the tangent of $f_T(\rho)$ would be common. This ensures phase coexistence, *i.e.* the chemical potentials match, $\mu_T(\rho_1) = \mu_T(\rho_2)$, because $\mu_T(\rho) = \partial_\rho f_T(\rho)$, and so do the pressures, $p_T(\rho_1) = p_T(\rho_2)$, because $p_T(\rho) = \mu_T(\rho)\rho - f_T(\rho)$. Ref. [18] extended the equation of state to $T > T_{\rm crit}$ by using splines that are convex, as is characteristic of single-phase systems. After having thus constructed $f_T(\rho)$ for a sufficient range of T and ρ, we may obtain the pressure, as well as the energy density $\varepsilon_T(\rho) = f_T(\rho) - T\partial_T f_T(\rho)$, by suitable interpolation and then tabulate the equation of state, $p_0(\varepsilon,\rho)$, on a convenient Cartesian lattice.

3. Fluid Dynamical Clumping

For our present investigation, we describe the evolution of the colliding system by ideal fluid dynamics, because dissipative effects are not expected to play a decisive role for the spinodal clumping [16]: Although the inclusion of viscosity generally tends to slow the growth, the dissipative mechanisms responsible for the viscous effects also lead to heat conduction which has the opposite effect and also enlarges the unstable region (from the isentropic to the isothermal boundary).

The basic equation of motion in ideal fluid dynamics expresses four-momentum conservation, $\partial_\mu T^\mu = 0$, where the stress tensor is given by

$$T^{\mu\nu}(x) = [p(x) + \varepsilon(x)]u^\mu(x)u^\nu(x) - p(x)g^{\mu\nu} \,, \tag{3.1}$$

where $u^\mu(x)$ is the four-velocity of the fluid. When taking account of the baryon current density, $N^\mu(x) = \rho(x)u^\mu(x)$, the basic equation of motion is supplemented by the continuity equation, $\partial_\mu N^\mu = 0$. These equations of motion are solved by means of the code SHASTA [17] in which the propagation in the three spatial dimensions is carried out consecutively.

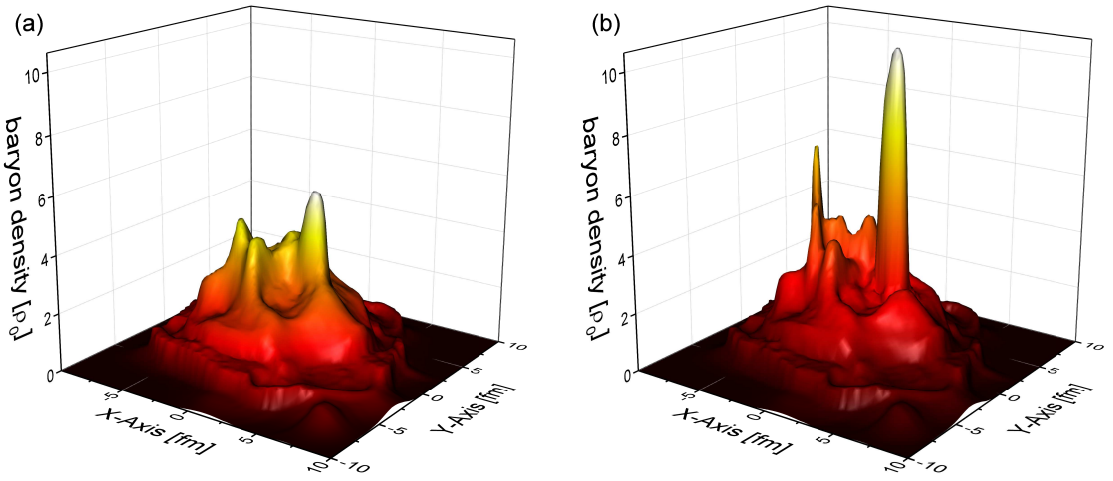

Figure 2: (a): The baryon density distribution in the transverse plane (at $z = 0$) at time $t = 2.5$ fm of a single event with the Maxwell constructed equation of state (b): The baryon density distribution in the transverse plane (at $z = 0$) at time $t = 2.5$ fm of the same event as in (a), this time with the unstable equation of state.

As mentioned above, a proper description of spinodal decomposition requires that finite-range effects be incorporated [5, 6]. Therefore, following Refs. [8, 16], we write the local pressure as

$$p(r) = p_0(\varepsilon(r), \rho(r)) - a^2 \varepsilon_s \frac{\rho(r)}{\rho_s} \nabla^2 \frac{\rho(r)}{\rho_s} \ , \tag{3.2}$$

where we recall that $p_0(\varepsilon, \rho)$ is the equation of state, the pressure in uniform matter characterized by ε and ρ. With $\rho_s = 0.153/\mathrm{fm}^3$ being the nuclear saturation density and $\varepsilon_s \approx m_N \rho_s$ the associated energy density, the gradient term is normalized such that its strength is conveniently governed by the length parameter a, which we will set to $a = 0.033$ [18] for the following results.

Uniform matter inside the spinodal region (where $v_s^2 < 0$) is mechanically unstable and density ripples of wave number k will be amplified at a rate $\gamma_k(\rho, \varepsilon)$. The spinodal growth rates can be extracted by following the time evolution of small harmonic perturbations of uniform matter. Thus, imposing periodic boundary conditions, we consider initial systems of the form

$$\rho(r) = \bar{\rho} + \delta\rho(0) \sin(kx) \ , \ \varepsilon(r) = \bar{\varepsilon} + \delta\varepsilon(0) \sin(kx) \ , \tag{3.3}$$

where $(\bar{\rho}, \bar{\varepsilon})$ lies inside the spinodal phase region and the amplitudes $\delta\rho(0)$ and $\delta\varepsilon(0)$ are suitably small. Because the frequency is purely imaginary, $\omega_k = \pm i\gamma_k$, the early time evolution of the amplitudes will consist of growing and decaying exponentials having equal weights (because the initial state (3.3) is prepared without any flow) [19],

$$\delta\rho(t) \approx \delta\rho(0) \cosh(\gamma_k t) \ , \ \delta\varepsilon(t) \approx \delta\varepsilon(0) \cosh(\gamma_k t) \ , \tag{3.4}$$

and it is then straightforward to extract the rate γ_k from the calculated amplitude growth.

This is illustrated in figure 1 for the phase point $(\bar{\rho}, \bar{\varepsilon}) = (6\rho_s, 10\varepsilon_s)$, which lies well inside the spinodal region, and using $(\delta\rho(0), \delta\varepsilon(0)) = (0.1\rho_s, 0.2\varepsilon_s)$. The subsequent time evolution is obtained with ideal fluid-dynamics (without the gradient term for this illustration) and the Fourier components of the density are extracted. The resulting time-dependent amplitudes $\delta\rho_k(t)$ are then

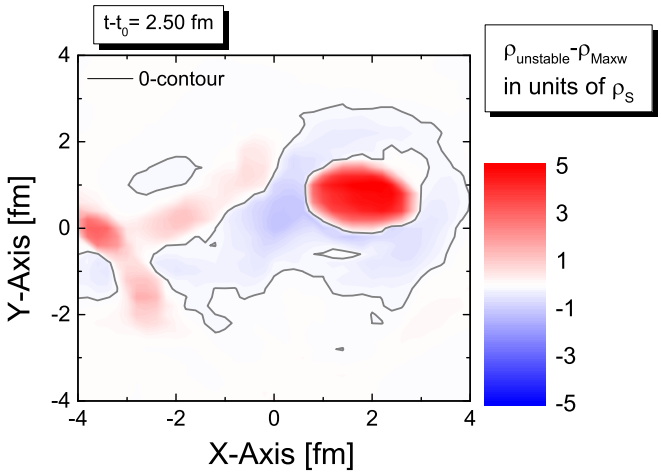

Figure 3: Density difference in the transverse plane (at $z = 0$) at time $t = 2.5$ fm of the events displayed in figure 3. The contour separates regions where the density is enhanced from regions where it is depleted.

fitted with the analytical form (3.4). As the figure brings out, the expected form is indeed produced, indicating that the numerical propagation of the unstable system is reliable.

4. Cluster Growth

In the present scenarios, spatial irregularities are present already in the initial state, whereas the fluid-dynamical propagation does not generate any spontaneous fluctuations in the course of the evolution (such fluctuations are generally produced at finite temperatures [20] but this refinement has not yet been incorporated into the fluid-dynamical transport treatments of nuclear collisions).

To estimate the effect of the non-equilibrium phase transition we create ensembles of initial states for different beam energies of collisions of lead nuclei using the UrQMD transport model [21, 22, 23]. For any given event, and at any given time, parts of the system may lie within the unstable or metastable region, and local density irregularities may then become amplified, whereas the rest of the matter is situated in a stable phase region where irregularities tend to erode. In order to ascertain the effect of those instabilities, we also carry out corresponding simulations with the one-phase Maxwell partner equation of state which contains no instabilities but is otherwise identical.

The difference in the density evolution is illustrated in figures (2a) and (2b). Both baryon density distributions, (a) and (b), are extracted after the same fluid dynamical evolution time $t = 2.5$ fm and from identical initial conditions. While in figure (2a) we used the Maxwell constructed equation of state, (2b) shows the reults with the unstable phase. It is clear that several regions with enhanced density appear when the system passes a region of instabilty. The difference of the two figures (2a) and (2b) is shown in figure (3), where the contour line separates regions with enhanced density from regions which are depleted of baryon number (due to the conservation of the total baryon number).

A convenient quantitative measure of the resulting degree of “clumping” in the system is pro-

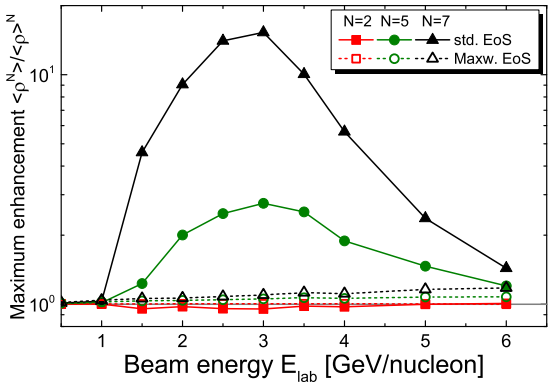

Figure 4: Mean maximum enhancement of the normalized density moments for $N = 7,5$ (squares, circles) as obtained for various energies using either the two-phase equation of state (solid) or its one-phase Maxwell partner (dashed).

vided by the moments of the baryon density density $\rho(r)$,

$$\langle \rho^N \rangle \equiv \frac{1}{A} \int \rho(r)^N \rho(r)\, d^3r \,, \tag{4.1}$$

where $A = \int \rho(r) d^3r$ is the total (net) baryon number. The corresponding normalized moments, $\langle \rho^N \rangle / \langle \rho \rangle^N$, are dimensionless and increase with the order N, for a given density distribution $\rho(r)$; the normalized moment for $N = 1$ is unity.

The degree of density clumping generated during a collision depends on how long time the bulk of the matter is exposed to the spinodal instabilities. The optimal situation occurs for collision energies that produce maximum bulk compressions lying well inside the unstable phase region because the instabilities may then act for the longest time [8, 16, 18]. At lower energies an ever smaller part of the system reaches instability and the resulting enhancements are smaller. Conversely, at higher energies the maximum compression occurs beyond the spinodal phase region and the system is exposed to the instabilities only during a relatively brief period during the subsequent expansion. For still higher energies the spinodal region is being missed entirely.

Figure 4 shows the (ensemble average) maximum enhancement achieved as a function of the beam energy for the two equations of state. The existence of an optimal collision energy is clearly brought out. While the presently employed equation of state suggests that this optimal range is $E_{\rm lab} \approx 2 - 4A\,{\rm GeV}$, it should be recognized that others may lead to different results.

To gain a more detailed understanding of the clumping phenomenon, we have studied the distribution of the clump sizes. Although the "clumps" tend to remain fairly diffuse, we may define their extension by means of a specified density cutoff, $\rho_{\rm min}$, and then extract the total net baryon number contained within the resulting volume. Figure 5 shows the size distribution obtained for a density cutoff of $\rho_{\rm min} = 7\rho_s$, for central lead-lead collisions at $3\,A\,{\rm GeV}$.

The initial size distribution is approximately exponential and that feature is well preserved during the evolution with the one-phase equation of state which produces negligible amplification. The spinodal instabilities in the two-phase equation of state leads to a preferential amplification of length scales near the optimum size, as is brought out by the difference between the two-phase

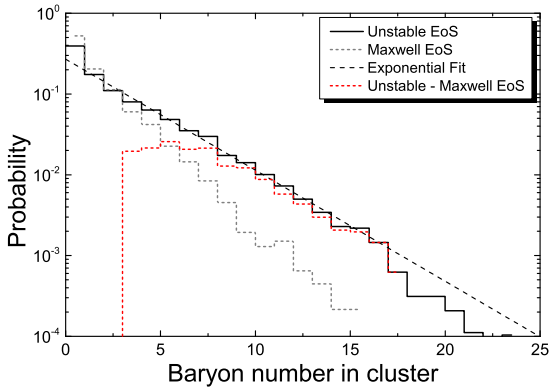

Figure 5: The size distribution of the density clumps produced in central lead-lead collisions at 3 AGeV using $\rho_{\rm min} = 7\rho_s$ to define the clump boundary. The solid histogram shows the distribution obtained for the two-phase equation of state and the solid line represents an exponential fit. The distribution obtained with the one-phase equation of state is shown by the dotted histogram and the difference between the two size distributions is also depicted.

size-distribution and the one obtained with the Maxwell partner; this difference peaks at clumps containing 5-8 baryons. Nevertheless, for a wide intermediate range, from about 3 to about 16, the resulting two-phase size distribution retains an approximately exponential appearance, but with a significantly gentler slope.

5. Summary

As reported recently [18], we have augmented an existing finite-density ideal fluid dynamics code with a gradient term and thereby obtained a transport model that is suitable for simulating nuclear collisions in the presence of a first-order phase transition. It describes both the temperature-dependent tension between coexisting phases and the amplification of the spinodal modes. Applying this novel model to lead-lead collisions, using an equation of state with a first-order phase transition, we found that the associated instabilities may cause significant amplification of initial density irregularities, relative to what would be obtained without the phase transition.

In particular, we extracted the density enhancement and the clump size distribution.

Perhaps most importantly our study supports the general existence of an optimal collision energy range within which the phase-transition instabilities have the largest effects on the dynamical evolution. Our results suggest that this energy corresponds to several GeV per nucleon of kinetic energy for a fixed-target configuration, a range that may be too low to access effectively at RHIC but which should match well with both FAIR and, especially, NICA.

6. Acknowledgments

We wish to acknowledge stimulating discussion with Volker Koch. This work was supported by the Office of Nuclear Physics in the U.S. Department of Energy's Office of Science under Contract No. DE-AC02-05CH11231; JS was supported in part by the Alexander von Humboldt Foundation as a Feodor Lynen Fellow.

References

[1] M. A. Stephanov, K. Rajagopal and E. V. Shuryak, Phys. Rev. Lett. **81**, 4816 (1998)

[2] B.I. Abelev *et al.*, Internal STAR Note SN0493, 2009: drupal.star.bnl.gov/STAR/starnotes/public/sn0493.

[3] B. Friman, C. Höhne, J. Knoll, S. Leupold, J. Randrup, R. Rapp, and P. Senger, *The CBM Physics Book*, (Springer, Berlin, 2010).

[4] A.N. Sissakian and A.S. Sorin, J. Phys. G **36**, 064069 (2009).

[5] Ph. Chomaz, M. Colonna, and J. Randrup, Phys. Rep. **389**, 263 (2004).

[6] J. Randrup, Phys. Rev. Lett. **92**, 122301 (2004)

[7] C. Sasaki, B. Friman and K. Redlich, Phys. Rev. Lett. **99**, 232301 (2007)

[8] J. Randrup, Phys. Rev. C **79**, 054911 (2009)

[9] C. Herold, M. Nahrgang, I. Mishustin and M. Bleicher, arXiv:1304.5372 [nucl-th].

[10] J. Randrup, Acta Phys. Hung. A **22**, 69 (2005).

[11] V. Koch, A. Majumder, and J. Randrup, Phys. Rev. C **72**, 064903 (2005).

[12] I. N. Mishustin, Phys. Rev. Lett. **82**, 4779 (1999)

[13] D. Bower and S. Gavin, Phys. Rev. C **64**, 051902 (2001)

[14] K. Paech, H. Stoecker and A. Dumitru, Phys. Rev. C **68**, 044907 (2003)

[15] M. Nahrgang, S. Leupold, C. Herold, and M. Bleicher, Phys. Rev. C **84**, 024912 (2011).

[16] J. Randrup, Phys. Rev. C **82**, 034902 (2010)

[17] D. H. Rischke, S. Bernard and J. A. Maruhn, Nucl. Phys. A **595**, 346 (1995)

[18] J. Steinheimer and J. Randrup, Phys. Rev. Lett. **109**, 212301 (2012)

[19] M. Colonna, Ph. Chomaz, and J. Randrup, Nucl. Phys. A **567**, 637 (1994).

[20] J. I. Kapusta, B. Muller and M. Stephanov, Phys. Rev. C **85**, 054906 (2012)

[21] M. Bleicher *et al.*, J. Phys. **G25**, 1859 (1999)

[22] S. A. Bass *et al.*, Prog. Part. Nucl. Phys. **41**, 255 (1998) [Prog. Part. Nucl. Phys. **41**, 225 (1998)]

[23] J. Steinheimer *et al.*, Phys. Rev. C **77**, 034901 (2008)